Journal of Sound and Vibration (2000) **235**(4), 539–565
doi:10.1006/jsvi.1999.2935, available online at http://www.idealibrary.com on IDEAL®

DEVELOPMENT OF SIMPLE MODELS FOR THE ELASTIC FORCES IN THE ABSOLUTE NODAL CO-ORDINATE FORMULATION

M. Berzeri and A. A. Shabana

Department of Mechanical Engineering, University of Illinois at Chicago,
842 *West Taylor Street, Chicago, IL* 60607-7022, *U.S.A.*

(*Received* 9 *July* 1999, *and in final form* 1 *December* 1999)

The objective of this study is to develop simple and accurate elastic force models that can be used in the absolute nodal co-ordinate formulation for the analysis of two-dimensional beams. These force models which account for the coupling between bending and axial deformations are derived using a continuum mechanics approach, without the need for introducing a local element co-ordinate system. Four new different force models that include different degrees of complexity are presented. It is shown that the vector of the elastic forces can be significantly simplified as compared to the elastic force model developed for the absolute nodal co-ordinate formulation using a local element frame [1]. Despite the simplicity of the new models, they account for elastic non-linearity in the strain–displacement relationship. Therefore, they lead to more accurate results as compared to the more complex models developed using the local frame method which does not account for the non-linearities in the strain–displacement relationships. Numerical results are presented in order to demonstrate the use of the new models and test their performances in the analysis of large deformations of flexible multibody systems.

1. INTRODUCTION

The absolute nodal co-ordinate formulation is a finite element non-incremental formulation recently introduced to study flexible multibody applications [1–3]. In this formulation, the nodal co-ordinates are defined in a global co-ordinate system. An important feature of this method is the use of global slopes instead of angles to define the orientation of the elements. Therefore, the absolute nodal co-ordinate formulation does not lead to linearization of the kinematic equations as in the case when infinitesimal rotations are used as nodal co-ordinates. Consequently, beam and plate elements, that are considered as non-isoparametric in the classical finite element formulations [4], become isoparametric when the absolute nodal co-ordinate formulation is used. Because of this property, good results have been obtained using the absolute nodal co-ordinate formulation in the cases of large rotation and large deformation problems [5]. The performance of this formulation was compared to the performance of the finite element corotational procedure [6] when flexible multibody systems are considered. The results obtained from this comparative study demonstrate the limitations of the incremental procedures in the analysis of flexible multibody systems which are characterized by high inertia forces and motion and velocity discontinuities.

In general, the absolute nodal co-ordinate formulation, due to the nature of the variables employed, leads to a simple expression for the inertia forces and a non-linear expression for

0022-460X/00/340539 + 27 $35.00/0

the elastic forces. One method used for formulating the elastic forces is to introduce a local element co-ordinate system for the convenience of defining the element deformations [1–3]. This approach, however, leads to a complex expression for the elastic forces. Another method which will be followed in this paper is to use a continuum mechanics approach without introducing a local element co-ordinate system. As demonstrated in this paper, the use of this approach leads to significant simplification in the vector of the elastic forces. Several elastic force models are developed in this investigation. Numerical results are presented in order to demonstrate the use of these models and test their performances in the analysis of simple flexible multibody applications.

It is important to point out that several models for the large deformation and rotation analysis were developed in the past [7–14]. Despite the fact that these investigations represent an important background, such investigations are not directly applicable to the subject of the study presented in this paper.

This paper is organized as follows. A brief review of the absolute nodal co-ordinate formulation is presented in section 2. In this section, the co-ordinates and shape function that will be repeatedly used in the following sections are defined. In section 3, the basic concepts and relationships used in the development of the force models presented in this paper are discussed. In section 4, three models for the elastic forces resulting from the longitudinal deformations are presented. The elastic force models due to the transverse deformations are presented in section 5. In section 6, an expression which is suitable for the numerical evaluation of the strain energy is provided. In section 7, the use of the force models and the strain energy models introduced in sections 4, 5 and 6 is demonstrated in the analysis of the large deformations of simple flexible multibody systems. In section 8, summary and conclusions drawn from the results of this investigation are presented.

2. ABSOLUTE NODAL CO-ORDINATE FORMULATION

In the absolute nodal co-ordinate formulation, the nodal co-ordinates of the elements are defined in a fixed inertial co-ordinate system, and consequently no co-ordinate transformation is required [1–3]. The element nodal co-ordinates represent global displacements and slopes, and no infinitesimal or finite rotations are used as nodal co-ordinates. Furthermore, no assumption on the magnitude of the element rotations is made. In the absolute nodal co-ordinate formulation, elements such as beams and plates that are considered in the finite element literature as non-isoparametric, can be treated as isoparametric elements.

The global position vector $\mathbf{r}$ of an arbitrary point P on the neutral axis of a two-dimensional beam element is defined in terms of the nodal co-ordinates and the element shape function, as shown in Figure 1, as

$$\mathbf{r} = \begin{bmatrix} r_1 \\ r_2 \end{bmatrix} = \mathbf{Se}, \tag{1}$$

where $\mathbf{S}$ is the global shape function which has a complete set of rigid-body modes, and $\mathbf{e}$ is the vector of element nodal co-ordinates:

$$\mathbf{e} = [e_1 \;\; e_2 \;\; e_3 \;\; e_4 \;\; e_5 \;\; e_6 \;\; e_7 \;\; e_8]^{\mathrm{T}}. \tag{2}$$

This vector of absolute nodal co-ordinates includes the global displacements

$$e_1 = r_1|_{x=0}, \quad e_2 = r_2|_{x=0}, \quad e_5 = r_1|_{x=l}, \quad e_6 = r_2|_{x=l}, \tag{3}$$

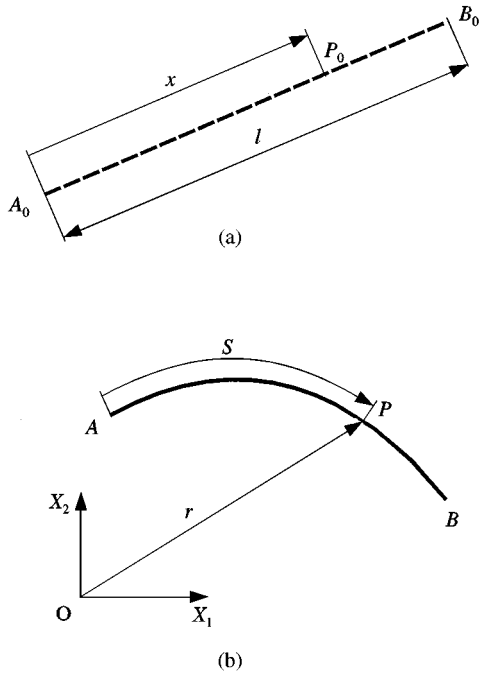

Figure 1. (a) Original and (b) current configurations in the absolute nodal co-ordinate formulation.

and the global slopes of the element nodes, that are defined as

$$e_3 = \left.\frac{\partial r_1}{\partial x}\right|_{x=0}, \quad e_4 = \left.\frac{\partial r_2}{\partial x}\right|_{x=0}, \quad e_7 = \left.\frac{\partial r_1}{\partial x}\right|_{x=l}, \quad e_8 = \left.\frac{\partial r_2}{\partial x}\right|_{x=l}. \tag{4}$$

Here, x is the co-ordinate of an arbitrary point on the element in the undeformed configuration, and l is the original length of the beam element (at point A, $x = 0$; while at point B, $x = l$, as shown in Figure 1). A cubic polynomial is employed to describe both components of the displacements. Therefore, the global shape function $\mathbf{S}$ can be written as

$$\mathbf{S} = \begin{bmatrix} s_1 & 0 & s_2 l & 0 & s_3 & 0 & s_4 l & 0 \\ 0 & s_1 & 0 & s_2 l & 0 & s_3 & 0 & s_4 l \end{bmatrix}, \tag{5}$$

where the functions $s_i = s_i(\xi)$ are defined as

$$s_1 = 1 - 3\xi^2 + 2\xi^3, \quad s_2 = \xi - 2\xi^2 + \xi^3, \quad s_3 = 3\xi^2 - 2\xi^3, \quad s_4 = \xi^3 - \xi^2, \tag{6}$$

and $\xi = x/l$. It can be shown that the preceding shape function contains a complete set of rigid-body modes that can describe arbitrary rigid-body translational and rotational displacements.

In the absolute nodal co-ordinate formulation, the use of slopes instead of rotations allows the representation of complex shapes using a small number of elements. For example, Figure 2 shows the configuration of one element whose original length is equal to 5 units as the vector of nodal co-ordinates, using the same units, is given by:

$$\mathbf{e} = [1{\cdot}5 \;\; 1{\cdot}5 \;\; -3 \;\; -2 \;\; -1 \;\; 1 \;\; -2 \;\; 3]^{\mathrm{T}}.$$

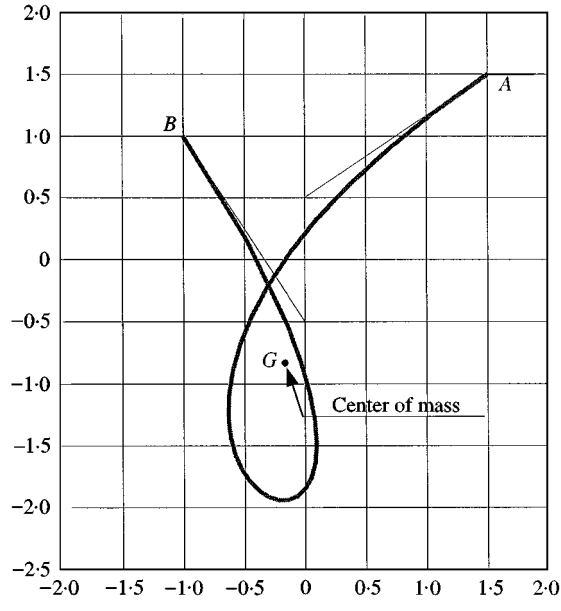

Figure 2. Configuration of a beam element with $l = 5$ and $\mathbf{e} = [1{\cdot}5\ \ 1{\cdot}5\ \ -3\ \ -2\ \ -1\ \ 1\ \ -2\ \ 3]^{\mathrm{T}}$.

Using the fact that the element presented in this section is isoparametric and using the principle of conservation of mass, which states that $\rho_0\,\mathrm{d}x = \rho\,\mathrm{d}s$ for a constant cross-sectional area A, one can show that the absolute nodal co-ordinate formulation leads to a constant mass matrix in the case of two-dimensional beam elements [2]. Here ρ is the mass density, s is the arc length and ρ_0 is the mass density in the undeformed configuration. The global position $\mathbf{r}_G$ of the center of mass G of an element is by definition given by

$$\mathbf{r}_G = \frac{1}{m}\int_V \rho\mathbf{r}\,\mathrm{d}V, \tag{7}$$

where m is the total mass of the element, and V is its volume. In the preceding equation, all the variables can be referred to the undeformed configuration, leading to

$$\mathbf{r}_G = \frac{1}{m}A\int_0^l \rho_0\mathbf{r}\,\mathrm{d}x, \tag{8}$$

where the cross-sectional area A of the element is assumed constant. For $\rho_0 = \text{constant}$, one obtains

$$\mathbf{r}_G = \begin{bmatrix} \frac{1}{2} & 0 & \frac{l}{12} & 0 & \frac{1}{2} & 0 & \frac{-l}{12} & 0 \\ 0 & \frac{1}{2} & 0 & \frac{l}{12} & 0 & \frac{1}{2} & 0 & \frac{-l}{12} \end{bmatrix}\mathbf{e}. \tag{9}$$

Hence, for arbitrary values of the nodal co-ordinates e_i and for an arbitrary length l of the beam element, the co-ordinates of the center of mass are given as a linear combination of the nodal co-ordinates, regardless of the amount of deformation. Figure 2 shows the center of mass G of the deformed element.

In order to develop the equations of motion of the element in the absolute nodal co-ordinate formulation, the vector $\mathbf{Q}_k$ of the elastic forces and the vector $\mathbf{Q}_e$ of the externally applied forces must be defined. The vector $\mathbf{Q}_k$ can be defined using the strain

energy U as

$$\mathbf{Q}_k = \left(\frac{\partial U}{\partial \mathbf{e}}\right)^{\mathrm{T}}, \tag{10}$$

while the vector $\mathbf{Q}_e$, that contains the generalized external forces, including the gravity force, can be defined using the virtual work as

$$\delta W_e = \mathbf{Q}_e^{\mathrm{T}} \delta \mathbf{e}. \tag{11}$$

Using the expressions of the kinetic energy, strain energy, and the virtual work, the dynamic equations of the finite element can be obtained in a matrix form as

$$\mathbf{M}\ddot{\mathbf{e}} + \mathbf{Q}_k = \mathbf{Q}_e. \tag{12}$$

As pointed out in reference [1], there are two methods that can be used to evaluate the non-linear elastic forces of the element in the absolute nodal co-ordinate formulation. In the first method, a local frame of reference is used for the element in order to define the element deformations. This approach leads to a complex expression for the elastic forces. The second method is based on a continuum mechanics approach which does not require the use of a local co-ordinate system for the finite element. In this investigation, several models based on the continuum mechanics approach are developed for the elastic forces of the elements in the absolute nodal co-ordinate formulation. The performance of these models is examined using numerical examples.

3. LARGE DEFORMATION BEAM MODEL

In this section, the basic concepts used in developing the beam models discussed in the following sections are presented. In these models, the effect of the rotary inertia and the effect of shear strain are neglected. Therefore, the beam element cross-sections are assumed to remain plane and perpendicular to the beam center line. The configuration of a beam element at time t can be defined using the parametric equation

$$\mathbf{r} = \mathbf{r}(x), \quad 0 \leqslant x \leqslant l, \tag{13}$$

where the vector $\mathbf{r}$ defines the co-ordinates of an arbitrary point on the beam axis, and x is considered as a parameter that represents the coordinate of the point in the undeformed configuration. The infinitesimal arc length is

$$\mathrm{d}s = \sqrt{\mathbf{r}'^{\mathrm{T}}\mathbf{r}'}\,\mathrm{d}x, \tag{14}$$

where

$$\mathbf{r}' = \frac{\mathrm{d}\mathbf{r}}{\mathrm{d}x}. \tag{15}$$

It follows that the length of the beam after deformation is given by

$$\int_l \mathrm{d}s = \int_0^l \sqrt{\mathbf{r}'^{\mathrm{T}}\mathbf{r}'}\,\mathrm{d}x. \tag{16}$$

The Serret–Frenet formulas [15] for the geometrical descriptions of curves provide the sufficient tools for the analysis that follows. The quantity $\sqrt{\mathbf{r}'^{\mathrm{T}}\mathbf{r}'}$ represents the deformation

gradient f for longitudinal deformations. This deformation gradient can be considered as the Cauchy–Green longitudinal strain which is defined here as

$$f = \mathrm{d}s/\mathrm{d}x. \tag{17}$$

Adopting a Lagrangian viewpoint, the longitudinal strain ε_l is defined by a relationship between the current and the original length of an infinitesimal segment of the beam as follows:

$$\mathrm{d}s^2 - \mathrm{d}x^2 = 2\,\mathrm{d}x\varepsilon_l\,\mathrm{d}x, \tag{18}$$

which implies that

$$\varepsilon_l = \tfrac{1}{2}(f^2 - 1) = \tfrac{1}{2}(\mathbf{r}'^{\mathrm{T}}\mathbf{r}' - 1). \tag{19}$$

Assuming isotropic materials, the strain energy due to the longitudinal deformation [16,17] can be written as

$$U_l = \frac{1}{2}\int_0^l EA\varepsilon_l^2\,\mathrm{d}x, \tag{20}$$

where E is Young's modulus. Note that in this development the problem of objectivity is solved by referring all the quantities to the undeformed configuration.

The effect of bending can be introduced using the equation [16]

$$M = EI\kappa, \tag{21}$$

where I is the second moment of area. The Serret–Frenet formulas give the following result for the curvature κ of a curve described in the parametric form of equation (13):

$$\kappa = \left|\frac{\mathrm{d}^2\mathbf{r}}{\mathrm{d}s^2}\right|. \tag{22}$$

In this case, the strain energy U_t due to bending can be written as

$$U_t = \frac{1}{2}\int_0^l EI\kappa^2\,\mathrm{d}x. \tag{23}$$

Therefore, the expression for the strain energy that accounts for both axial and bending effects is

$$U = U_l + U_t = \frac{1}{2}\int_0^l [EA\varepsilon_l^2 + EI\kappa^2]\,\mathrm{d}x. \tag{24}$$

Note that the curvature of equation (22) can also be written as [15]

$$\kappa = \frac{|\mathbf{r}' \times \mathbf{r}''|}{|\mathbf{r}'|^3}. \tag{25}$$

In this equation, both the numerator and the denominator depend on the amount of longitudinal deformation that may also influence the bending deformations. However, in the literature, the denominator in equation (25) is often considered equal to one, since the curvature is approximated with the second spatial derivative of the transverse deflection of the beam [18,19]. In section 5, two transverse deflection force models will be presented; one

model considers the effects of the longitudinal deformation on the curvature, while in the other model this effect is neglected.

For two-dimensional problems, equation (25) can be written as

$$\kappa = \frac{\mathbf{r}''^{\mathrm{T}}\tilde{\mathbf{I}}\mathbf{r}'}{|\mathbf{r}'^{\mathrm{T}}\mathbf{r}'|^{3/2}} = \frac{\mathbf{r}''^{\mathrm{T}}\tilde{\mathbf{I}}\mathbf{r}'}{f^3}, \tag{26}$$

where

$$\tilde{\mathbf{I}} = \begin{bmatrix} 0 & -1 \\ 1 & 0 \end{bmatrix}. \tag{27}$$

The expression of the curvature becomes much simpler in the special case of small longitudinal deformations. In this case, when $f \simeq 1$, equation (22) yields

$$\kappa \simeq \left| \frac{\mathrm{d}^2\mathbf{r}}{\mathrm{d}x^2} \right| = |\mathbf{r}''|, \tag{28}$$

and this assumptions leads to a significant simplification of the equation of the strain energy. Note that this formula holds in the case of small longitudinal deformations; no assumption has been made with regard to the amount of the transverse deformation.

4. LONGITUDINAL FORCE MODELS

In this section, several longitudinal force models that can be used in the absolute nodal co-ordinate formulation are presented. Despite the fact that these models account for the elastic non-linearities as described by the Green–Lagrangian strain measure, two of them lead to expressions simpler than the one obtained by the model developed using the local element co-ordinate system and a linear strain–displacement relationship.

For convenience, the following matrices are defined:

$$\mathbf{S}_l = \mathbf{S}'^{\mathrm{T}}\mathbf{S}' = \frac{1}{l^2}\mathbf{S}_{,\xi}^{\mathrm{T}}\mathbf{S}_{,\xi}, \quad \bar{\mathbf{S}}_l = \int_0^1 \mathbf{S}_l \,\mathrm{d}\xi, \tag{29,30}$$

where $\mathbf{S}_{,\xi}$ is the derivative of the shape function $\mathbf{S}$ defined in equation (5) with respect to the dimensionless parameter $\xi = x/l$. Using equation (1), one obtains

$$\mathbf{r}'^{\mathrm{T}}\mathbf{r}' = \mathbf{e}^{\mathrm{T}}\mathbf{S}'^{\mathrm{T}}\mathbf{S}'\mathbf{e}. \tag{31}$$

Substituting equation (31) into equation (19), and using the definition of $\mathbf{S}_l$ given by equation (29), the longitudinal strain can be written as

$$\varepsilon_l = \tfrac{1}{2}(\mathbf{e}^{\mathrm{T}}\mathbf{S}_l\mathbf{e} - 1). \tag{32}$$

From this equation it is clear that

$$\left(\frac{\partial \varepsilon_l}{\partial \mathbf{e}}\right)^{\mathrm{T}} = \mathbf{S}_l\mathbf{e}, \tag{33}$$

and the vector $\mathbf{Q}_l$ of the generalized elastic forces due to the longitudinal deformation can be defined as

$$\mathbf{Q}_l = \left(\frac{\partial U_l}{\partial \mathbf{e}}\right)^{\mathrm{T}} = \int_0^l EA\varepsilon_l \mathbf{S}_l \mathbf{e}\, \mathrm{d}x, \tag{34}$$

which can also be written as

$$\mathbf{Q}_l = \mathbf{K}_l \mathbf{e}, \tag{35}$$

where the stiffness matrix is given by

$$\mathbf{K}_l = \int_0^l EA\varepsilon_l \mathbf{S}_l\, \mathrm{d}x. \tag{36}$$

Depending on the way the strain ε_l is presented in the preceding equation, different longitudinal force models can be obtained. In the remainder of this section, three models L1, L2 and L3 are discussed.

4.1. FIRST MODEL L1

It is clear that if ε_l is assumed to be constant throughout the beam element, it is then possible to factor it out of the integral sign of equation (34). Using this assumption and assuming that E and A are constants, the vector of generalized elastic forces due to the longitudinal deformation can be written as

$$\mathbf{Q}_l = EAl\bar{\varepsilon}_l \int_0^1 \mathbf{S}_l \mathbf{e}\, \mathrm{d}\xi = EAl\bar{\varepsilon}_l \bar{\mathbf{S}}_l \mathbf{e}. \tag{37}$$

In this equation, $\bar{\varepsilon}_l$ is the average longitudinal strain along the element, and in the case of small deformations it can be simply approximated as

$$\bar{\varepsilon}_l = \frac{d - l}{l}, \tag{38}$$

where d is the distance between the nodes of the elements defined as

$$d = \sqrt{(e_5 - e_1)^2 + (e_6 - e_2)^2}. \tag{39}$$

Using the constant strain assumption, the stiffness matrix $\mathbf{K}_l$ defined by equation (35) can be written explicitly as

$$\mathbf{K}_l = \frac{EA}{l}\bar{\varepsilon}_l \begin{bmatrix} \frac{6}{5} & 0 & \frac{l}{10} & 0 & \frac{-6}{5} & 0 & \frac{l}{10} & 0 \\ & \frac{6}{5} & 0 & \frac{l}{10} & 0 & \frac{-6}{5} & 0 & \frac{l}{10} \\ & & \frac{2l^2}{15} & 0 & \frac{-l}{10} & 0 & \frac{-l^2}{30} & 0 \\ & & & \frac{2l^2}{15} & 0 & \frac{-l}{10} & 0 & \frac{-l^2}{30} \\ & & & & \frac{6}{5} & 0 & \frac{-l}{10} & 0 \\ & sym & & & & \frac{6}{5} & 0 & \frac{-l}{10} \\ & & & & & & \frac{2l^2}{15} & 0 \\ & & & & & & & \frac{2l^2}{15} \end{bmatrix}. \tag{40}$$

This matrix, which has a very simple structure, is very similar to the stiffness matrix obtained in reference [19] when a first non-linear formulation is adopted for the elastic forces. As it will be shown in section 6, the simplicity of the first model leads to significant reduction in the computer time when multibody systems are simulated.

4.2. SECOND MODEL L2

Recall that the stiffness matrix of equation (40) is obtained using the assumption that the longitudinal strain remains constant throughout the finite element. Now this assumption is relaxed, and in order to find a general expression for the longitudinal strain, the vector $\mathbf{e}$ of nodal co-ordinates is written as the sum of two vectors,

$$\mathbf{e} = \mathbf{e}_r + \mathbf{e}_f, \tag{41}$$

where $\mathbf{e}_r$ represents an arbitrary rigid-body displacement,

$$\mathbf{e}_r = [x \;\; y \;\; c \;\; s \;\; x + lc \;\; y + ls \;\; c \;\; s]^{\mathrm{T}}, \tag{42}$$

and $\mathbf{e}_f$ is the result of the difference $\mathbf{e} - \mathbf{e}_r$. In equation (42), x and y are arbitrary rigid-body translations, and c and s stand for $\cos\theta$ and $\sin\theta$, respectively, where θ represents an arbitrary rigid-body rotation. One can easily show that

$$\mathbf{e}_r^{\mathrm{T}}\mathbf{S}_l\mathbf{e}_r = 1.$$

Note that, for small deformations, the quantity $\mathbf{e}^{\mathrm{T}}\mathbf{S}_l\mathbf{e}$ is very close to one, and the right-hand side of equation (32) can be difficult to numerically determine with good accuracy. However, with the use of the preceding identity, the longitudinal strain becomes

$$\varepsilon_l = \tfrac{1}{2}(\mathbf{e} - \mathbf{e}_r)^{\mathrm{T}}\mathbf{S}_l(\mathbf{e} + \mathbf{e}_r), \tag{43}$$

which shows that, with a convenient choice for $\mathbf{e}_r$, the strain ε_l can be accurately determined.

The vector of generalized elastic forces due to the longitudinal deformation is given by equation (35), where the matrix $\mathbf{K}_l$, assuming that E and A are constant, is

$$\mathbf{K}_l = EAl\int_0^1 \varepsilon_l\mathbf{S}_l\,\mathrm{d}\xi. \tag{44}$$

Since $\mathbf{e}_r$ in equation (43) is arbitrary, one may conveniently choose $\mathbf{e}_r = [0\ 0\ 1\ 0\ l\ 0\ 1\ 0]^{\mathrm{T}}$. Using this vector and equation (43), the stiffness matrix of equation (44) can be explicitly written as

$$\mathbf{K}_l = \frac{EA}{l}\begin{bmatrix} \mathscr{A} & 0 & \mathscr{B} & 0 & -\mathscr{A} & 0 & \mathscr{C} & 0 \\ & \mathscr{A} & 0 & \mathscr{B} & 0 & -\mathscr{A} & 0 & \mathscr{C} \\ & & \mathscr{D} & 0 & -\mathscr{B} & 0 & \mathscr{E} & 0 \\ & & & \mathscr{D} & 0 & -\mathscr{B} & 0 & \mathscr{E} \\ & & & & \mathscr{A} & 0 & -\mathscr{C} & 0 \\ & sym & & & & \mathscr{A} & 0 & -\mathscr{C} \\ & & & & & & \mathscr{F} & 0 \\ & & & & & & & \mathscr{F} \end{bmatrix}, \tag{45}$$

which contains six independent elements $\mathscr{A}$, $\mathscr{B}$, $\mathscr{C}$, $\mathscr{D}$, $\mathscr{E}$, and $\mathscr{F}$. In order to write the expression of these six components, it is convenient to introduce the quantities

$$d_x = e_5 - e_1, \quad d_y = e_6 - e_2, \tag{46}$$

where $d = \sqrt{d_x^2 + d_y^2}$ is also defined by equation (39), and

$$a_x = le_3, \quad a_y = le_4, \quad a = \sqrt{a_x^2 + a_y^2}, \tag{47}$$

$$b_x = le_7, \quad b_y = le_8, \quad b = \sqrt{b_x^2 + b_y^2}. \tag{48}$$

Using these definitions, the six independent elements that appear in equation (45) can be written as

$$\mathscr{A} = \frac{3}{70l^2}(a^2 + b^2 - 14l^2 - 6a_xd_x - 6b_xd_x - 6a_yd_y - 6b_yd_y + 24d^2), \tag{49}$$

$$\mathscr{B} = \frac{1}{280l}(b^2 - a^2 + 2a_xb_x + 2a_yb_y - 14l^2 - 24a_xd_x - 24a_yd_y + 36d^2), \tag{50}$$

$$\mathscr{C} = \frac{1}{280l}(a^2 - b^2 + 2a_xb_x + 2a_yb_y - 14l^2 - 24b_xd_x - 24b_yd_y + 36d^2), \tag{51}$$

$$\mathscr{D} = \tfrac{1}{420}(12a^2 + b^2 - 3a_xb_x - 3a_yb_y - 28l^2 + 3a_xd_x - 3b_xd_x + 3a_yd_y - 3b_yd_y + 18d^2), \tag{52}$$

$$\mathscr{E} = \tfrac{-1}{840}(3a^2 + 3b^2 - 4a_xb_x - 4a_yb_y - 14l^2 + 6a_xd_x + 6b_xd_x + 6a_yd_y + 6b_yd_y), \tag{53}$$

$$\mathscr{F} = \tfrac{1}{420}(a^2 + 12b^2 - 3a_xb_x - 3a_yb_y - 28l^2 - 3a_xd_x + 3b_xd_x - 3a_yd_y + 3b_yd_y + 18d^2). \tag{54}$$

The matrix $\mathbf{K}_l$ defined by equation (45) becomes the null matrix in case of rigid-body displacements. This result has been obtained without using any simplification in the development of this stiffness matrix.

Note that the matrix $\mathbf{K}_l$ is not unique. It is possible to follow a different route to evaluate the vector of generalized elastic forces due to longitudinal deformations. Since ε_l is a scalar, the vector $\mathbf{Q}_l$ of equation (34) can be written as

$$\mathbf{Q}_l = \int_0^l EA(\mathbf{S}_l\mathbf{e})\varepsilon_l \,\mathrm{d}x. \tag{55}$$

Using the definition of longitudinal strain given by equation (32), one obtains

$$\mathbf{Q}_l = \frac{1}{2}\int_0^l EA(\mathbf{S}_l\mathbf{e})(\mathbf{e}^{\mathrm{T}}\mathbf{S}_l\mathbf{e} - 1)\,\mathrm{d}x. \tag{56}$$

Assuming E and A as constants, the stiffness matrix $\mathbf{K}_l$ can be written as

$$\mathbf{K}_l = \frac{1}{2}EAl\left[\int_0^1 (\mathbf{S}_l\mathbf{e}\mathbf{e}^{\mathrm{T}}\mathbf{S}_l)\,\mathrm{d}\xi - \int_0^1 \mathbf{S}_l\,\mathrm{d}\xi\right], \tag{57}$$

which remains symmetric. However, it can be shown that the stiffness matrix of the preceding equation is a full matrix whose elements are quadratic functions of the nodal co-ordinates e_i.

4.3. THIRD MODEL L3

The six independent elements $\mathscr{A}$, $\mathscr{B}$, $\mathscr{C}$, $\mathscr{D}$, $\mathscr{E}$, and $\mathscr{F}$ of the stiffness matrix $\mathbf{K}_l$ defined by equation (45) can be simplified in the case of small deformations. Using the first element as an example, it is possible to show that $\mathscr{A}$ is the sum of two quantities that are small when the deformation within the element becomes infinitesimal. Introducing an average strain $\bar{\varepsilon}_l$ as a measure of the deformation, it is possible to write

$$\mathscr{A} = O_A(\bar{\varepsilon}_l) + o_A(\bar{\varepsilon}_l), \tag{58}$$

where

$$O_A = \frac{3}{5}\frac{d^2 - l^2}{l^2} + \frac{3}{35}\frac{2d^2 - a^2 - b^2}{l^2} \tag{59}$$

and

$$o_A = \frac{9}{70}\frac{(a_x - d_x)^2 + (b_x - d_x)^2 + (a_y - d_y)^2 + (b_y - d_y)^2}{l^2}. \tag{60}$$

Here the usual mathematical notation has been considered, such that $O_A(\bar{\varepsilon}_l)$ denotes an infinitesimal quantity of the same order as $\bar{\varepsilon}_l$, while $o_A(\bar{\varepsilon}_l)$ is an infinitesimal quantity of higher order. To prove this fact, it is enough to show that when $\bar{\varepsilon}_l \to 0$, each term in o_A becomes the square of an infinitesimal quantity, which can be neglected. Using a similar argument for each element of the matrix given by equation (45), one can show that the elements $\mathscr{A}$, $\mathscr{B}$, $\mathscr{C}$, $\mathscr{D}$, $\mathscr{E}$, and $\mathscr{F}$ can be written as

$$\mathscr{A} = \tfrac{6}{5}\varepsilon_M + \tfrac{6}{35}(-\varepsilon_A + 2\varepsilon_M - \varepsilon_B), \tag{61}$$

$$\mathscr{B} = \frac{l}{10}\varepsilon_M + \frac{l}{70}(-6\varepsilon_A + 5\varepsilon_M + \varepsilon_B), \tag{62}$$

$$\mathscr{C} = \frac{l}{10}\varepsilon_M + \frac{l}{70}(\varepsilon_A + 5\varepsilon_M - 6\varepsilon_B), \tag{63}$$

$$\mathscr{D} = \frac{2l^2}{15}\varepsilon_M + \frac{l^2}{105}(6\varepsilon_A - 5\varepsilon_M - \varepsilon_B), \tag{64}$$

$$\mathscr{E} = -\frac{l^2}{30}\varepsilon_M - \frac{l^2}{210}(2\varepsilon_A - 4\varepsilon_M + 2\varepsilon_B), \tag{65}$$

$$\mathscr{F} = \frac{2l^2}{15}\varepsilon_M + \frac{l^2}{105}(-\varepsilon_A - 5\varepsilon_M + 6\varepsilon_B), \tag{66}$$

where

$$\varepsilon_M = \frac{d - l}{l}, \quad \varepsilon_A = \frac{a - l}{l}, \quad \varepsilon_B = \frac{b - l}{l}. \tag{67}$$

The elements $\mathscr{A}$, $\mathscr{B}$, $\mathscr{C}$, $\mathscr{D}$, $\mathscr{E}$, and $\mathscr{F}$ of equations (61)–(66) are written as the sum of two terms, where only the first term is important when the variations in the longitudinal deformation within the element are small. In this case, one obtains the stiffness matrix of

Model L1. However, the variations in the longitudinal deformation within the elements are not always small as in the case in some applications including the simple free falling pendulum example discussed in section 7. Therefore, it is important to consider the actual distribution of the deformation within the element length. Equations (61)–(66) show that, in the case of small deformations, only the three quantities ε_M, ε_A and ε_B defined by equation (67) can be used to represent the distribution of the longitudinal strain. Using these three quantities, the stiffness matrix $\mathbf{K}_l$ can be written as

$$\mathbf{K}_l = \mathbf{K}_{lM} + \mathbf{K}_{lA} + \mathbf{K}_{lB}, \tag{68}$$

where

$$\mathbf{K}_{lM} = \frac{EA}{l}\varepsilon_M \begin{bmatrix} \frac{54}{35} & 0 & \frac{12l}{70} & 0 & \frac{-54}{35} & 0 & \frac{12l}{70} & 0 \\ & \frac{54}{35} & 0 & \frac{12l}{70} & 0 & \frac{-54}{35} & 0 & \frac{12l}{70} \\ & & \frac{9l^2}{105} & 0 & \frac{-12l}{70} & 0 & \frac{-l^2}{70} & 0 \\ & & & \frac{9l^2}{105} & 0 & \frac{-12l}{70} & 0 & \frac{-l^2}{70} \\ & & & & \frac{54}{35} & 0 & \frac{-12l}{70} & 0 \\ & sym & & & & \frac{54}{35} & 0 & \frac{-12l}{70} \\ & & & & & & \frac{9l^2}{105} & 0 \\ & & & & & & & \frac{9l^2}{105} \end{bmatrix}, \tag{69}$$

$$\mathbf{K}_{lA} = \frac{EA}{l}\varepsilon_A \begin{bmatrix} \frac{-6}{35} & 0 & \frac{-6l}{70} & 0 & \frac{6}{35} & 0 & \frac{l}{70} & 0 \\ & \frac{-6}{35} & 0 & \frac{-6l}{70} & 0 & \frac{6}{35} & 0 & \frac{l}{70} \\ & & \frac{6l^2}{105} & 0 & \frac{6l}{70} & 0 & \frac{-l^2}{105} & 0 \\ & & & \frac{6l^2}{105} & 0 & \frac{6l}{70} & 0 & \frac{-l^2}{105} \\ & & & & \frac{-6}{35} & 0 & \frac{-l}{70} & 0 \\ & sym & & & & \frac{-6}{35} & 0 & \frac{-l}{70} \\ & & & & & & \frac{-l^2}{105} & 0 \\ & & & & & & & \frac{-l^2}{105} \end{bmatrix}, \tag{70}$$

$$\mathbf{K}_{lB} = \frac{EA}{l}\varepsilon_B \begin{bmatrix} \frac{-6}{35} & 0 & \frac{l}{70} & 0 & \frac{6}{35} & 0 & \frac{-6l}{70} & 0 \\ & \frac{-6}{35} & 0 & \frac{l}{70} & 0 & \frac{6}{35} & 0 & \frac{-6l}{70} \\ & & \frac{-l^2}{105} & 0 & \frac{-l}{70} & 0 & \frac{-l^2}{105} & 0 \\ & & & \frac{-l^2}{105} & 0 & \frac{-l}{70} & 0 & \frac{-l^2}{105} \\ & & & & \frac{-6}{35} & 0 & \frac{6l}{70} & 0 \\ & sym & & & & \frac{-6}{35} & 0 & \frac{6l}{70} \\ & & & & & & \frac{6l^2}{105} & 0 \\ & & & & & & & \frac{6l^2}{105} \end{bmatrix}. \tag{71}$$

It can be shown that the application of this force model to simple static problems leads to the correct analytical solution.

Model L3 is slightly more complex than Model L1, but it can be used in the general case of small deformations, which is the case in many engineering applications. Note that in developing this model, no assumptions are introduced except the small deformation

assumption. In the problems where this assumption is not justified, the use of Model L2 becomes necessary, with the drawback of an increased simulation time. The advantages and drawbacks of the three models presented in this section will be discussed in section 6.

5. TRANSVERSE FORCE MODELS

In this section, two simple models for the elastic forces associated with the transverse deformation are developed for the absolute nodal coordinate formulation. The first Model T1 can be used when the longitudinal deformation is small. The second Model T2, on the other hand, can be used in the case of large longitudinal and transverse deformations.

5.1. FIRST MODEL T1

For this model, the simplified expression of the curvature given by equation (28) is considered. Using equation (2), one obtains

$$\kappa^2 = \mathbf{e}^{\mathrm{T}}\mathbf{S}''^{\mathrm{T}}\mathbf{S}''\mathbf{e}. \tag{72}$$

The strain energy defined by equation (23) in this case can be written as

$$U_t = \tfrac{1}{2}\mathbf{e}^{\mathrm{T}}\mathbf{K}_t\mathbf{e}, \tag{73}$$

where the stiffness matrix $\mathbf{K}_t$ is constant and defined as

$$\mathbf{K}_t = \int_0^l EI\mathbf{S}''^{\mathrm{T}}\mathbf{S}''\,\mathrm{d}x. \tag{74}$$

Assuming E and I are constant and using the shape function of equation (5), the stiffness matrix $\mathbf{K}_t$ can be written explicitly as

$$\mathbf{K}_t = \frac{EI}{l^3}\begin{bmatrix} 12 & 0 & 6l & 0 & -12 & 0 & 6l & 0 \\ & 12 & 0 & 6l & 0 & -12 & 0 & 6l \\ & & 4l^2 & 0 & -6l & 0 & 2l^2 & 0 \\ & & & 4l^2 & 0 & -6l & 0 & 2l^2 \\ & & & & 12 & 0 & -6l & 0 \\ & sym & & & & 12 & 0 & -6l \\ & & & & & & 4l^2 & 0 \\ & & & & & & & 4l^2 \end{bmatrix}. \tag{75}$$

This constant matrix is similar to the stiffness matrix used in linear structural dynamics, and has also been obtained by Takahashi and Shimizu [20]. The vector of elastic forces is then given by

$$\mathbf{Q}_t = \mathbf{K}_t\mathbf{e}. \tag{76}$$

5.2. SECOND MODEL T2

When the longitudinal deformation is not small, the use of equation (28) is no longer justified, as it is clear from equation (26) that shows that the curvature can significantly

change in the case of a large longitudinal deformation. In this case, equation (26) must be used. The numerator of this equation, written in terms of the absolute nodal co-ordinates, becomes

$$\mathbf{r}'^{\mathrm{T}}\tilde{\mathbf{I}}\mathbf{r}'' = \mathbf{e}^{\mathrm{T}}\hat{\mathbf{S}}_t\mathbf{e}, \tag{77}$$

where the matrix $\hat{\mathbf{S}}_t$ is defined as

$$\hat{\mathbf{S}}_t = \mathbf{S}'^{\mathrm{T}}\tilde{\mathbf{I}}\mathbf{S}'' = \frac{1}{l^3}\mathbf{S}_{,\xi}^{\mathrm{T}}\tilde{\mathbf{I}}\mathbf{S}_{,\xi\xi}. \tag{78}$$

Note that the curvature is a scalar, and it is equal to its transpose, so that the following relation holds:

$$\mathbf{e}^{\mathrm{T}}\hat{\mathbf{S}}_t\mathbf{e} = \mathbf{e}^{\mathrm{T}}\mathbf{S}_t\mathbf{e}, \tag{79}$$

where the symmetric matrix $\mathbf{S}_t$ has been introduced,

$$\mathbf{S}_t = \tfrac{1}{2}(\hat{\mathbf{S}}_t + \hat{\mathbf{S}}_t^{\mathrm{T}}). \tag{80}$$

The matrix $\mathbf{S}_t$ is a sparse matrix with a very simple structure. Hence, without using any approximation, the curvature can be written as

$$\kappa = \frac{\mathbf{e}^{\mathrm{T}}\mathbf{S}_t\mathbf{e}}{f^3}. \tag{81}$$

This equation can be substituted into the strain energy expression U_t of equation (23) in order to determine the elastic forces due to the transverse deformation. Equation (81), however, will lead to a complex expression for the elastic forces. This expression can be significantly simplified if the longitudinal deformation within the element is assumed constant in developing the transverse elastic forces. In this case, the deformation gradient f is assumed equal to a constant value $\bar{f}$:

$$\frac{\mathrm{d}s}{\mathrm{d}x} = \bar{f} = \text{const}. \tag{82}$$

It follows that

$$\frac{\mathrm{d}^2\mathbf{r}}{\mathrm{d}s^2} = \frac{1}{\bar{f}^2}\mathbf{r}'', \tag{83}$$

and consequently

$$\kappa^2 = \frac{1}{\bar{f}^4}\mathbf{e}^{\mathrm{T}}\mathbf{S}''^{\mathrm{T}}\mathbf{S}''\mathbf{e}. \tag{84}$$

Using the preceding equation, the definition of the strain energy U_t of equation (23) and the shape function of equation (5), it can be shown that the vector of the elastic forces due to the transverse deformation is given by

$$\mathbf{Q}_t = \left(\frac{\partial U_t}{\partial \mathbf{e}}\right)^{\mathrm{T}} = EIl\left[\frac{1}{\bar{f}^4}\int_0^1 \mathbf{S}''^{\mathrm{T}}\mathbf{S}''\,\mathrm{d}\xi - \frac{2}{\bar{f}^2}\int_0^1 \kappa^2\,\mathrm{d}\xi\,\bar{\mathbf{S}}_l\right]\mathbf{e}. \tag{85}$$

In order to obtain equation (85), the following definition of the average deformation gradient $\bar{f}$ has been used:

$$\bar{f} = \sqrt{\int_0^1 f^2 \, \mathrm{d}\xi} = \sqrt{\int_0^1 \mathbf{r}'^{\mathrm{T}} \mathbf{r}' \, \mathrm{d}\xi} = \sqrt{\mathbf{e}^{\mathrm{T}} \bar{\mathbf{S}}' \mathbf{e}}. \tag{86}$$

In a similar manner, one can define an average curvature as

$$\bar{\kappa} = \sqrt{\int_0^1 \kappa^2 \, \mathrm{d}\xi} = \frac{1}{\bar{f}^2} \sqrt{\int_0^1 \mathbf{r}''^{\mathrm{T}} \mathbf{r}'' \, \mathrm{d}\xi} = \frac{1}{\bar{f}^2} \sqrt{\mathbf{e}^{\mathrm{T}} \left(\int_0^1 \mathbf{S}''^{\mathrm{T}} \mathbf{S}'' \, \mathrm{d}\xi \right) \mathbf{e}}. \tag{87}$$

Equation (85) leads to the vector of elastic forces,

$$\mathbf{Q}_t = (\mathbf{K}_{t1} + \mathbf{K}_{t2})\mathbf{e}, \tag{88}$$

where

$$\mathbf{K}_{t1} = \frac{EI}{l^3} \frac{1}{\bar{f}^4} \begin{bmatrix} 12 & 0 & 6l & 0 & -12 & 0 & 6l & 0 \\ & 12 & 0 & 6l & 0 & -12 & 0 & 6l \\ & & 4l^2 & 0 & -6l & 0 & 2l^2 & 0 \\ & & & 4l^2 & 0 & -6l & 0 & 2l^2 \\ & & & & 12 & 0 & -6l & 0 \\ & sym & & & & 12 & 0 & -6l \\ & & & & & & 4l^2 & 0 \\ & & & & & & & 4l^2 \end{bmatrix}, \tag{89}$$

and

$$\mathbf{K}_{t2} = -2 \frac{EI}{l} \frac{\bar{\kappa}^2}{\bar{f}^2} \begin{bmatrix} \frac{6}{5} & 0 & \frac{l}{10} & 0 & \frac{-6}{5} & 0 & \frac{l}{10} & 0 \\ & \frac{6}{5} & 0 & \frac{l}{10} & 0 & \frac{-6}{5} & 0 & \frac{l}{10} \\ & & \frac{2l^2}{15} & 0 & \frac{-l}{10} & 0 & \frac{-l^2}{30} & 0 \\ & & & \frac{2l^2}{15} & 0 & \frac{-l}{10} & 0 & \frac{-l^2}{30} \\ & & & & \frac{6}{5} & 0 & \frac{-l}{10} & 0 \\ & sym & & & & \frac{6}{5} & 0 & \frac{-l}{10} \\ & & & & & & \frac{2l^2}{15} & 0 \\ & & & & & & & \frac{2l^2}{15} \end{bmatrix}. \tag{90}$$

The matrix $\mathbf{K}_{t1}$ of equation (89) is very similar to the matrix $\mathbf{K}_t$ of equation (75); $\mathbf{K}_{t1}$ reduces to $\mathbf{K}_t$ in the case of small deformations, when $\bar{f} \simeq 1$. The matrix $\mathbf{K}_{t2}$ contains the terms related to the derivative $\partial \bar{f} / \partial \mathbf{e}$; these terms appear when one differentiates equation (84) with respect to the vector of nodal coordinates. In the case of small deformations, the curvature is small ($\bar{\kappa} \simeq 0$), and $\mathbf{K}_{t2}$ reduces to the null matrix.

Model T2 for the elastic forces due to transverse deformations should be used with Model L2 presented in the preceding section to study the general case of large deformations. In order to meet the assumption of constant longitudinal deformation within the finite element, a sufficient number of elements should also be used.

6. EXPRESSION OF THE STRAIN ENERGY

The strain energy expression presented in section 2 is used in this investigation to determine the vector of the elastic forces in the absolute nodal co-ordinate formulation. The vector of the elastic forces was defined as

$$\mathbf{Q} = \left(\frac{\partial U}{\partial \mathbf{e}}\right)^{\mathrm{T}} = \mathbf{K}\mathbf{e},$$

where U is the strain energy, and $\mathbf{K}$ is the stiffness matrix. During the simulation of the large deformations, one may be interested in calculating the strain energy of the elements. This feature is available in many finite element codes, and it is the purpose of this section to develop an expression for the strain energy U in the absolute nodal co-ordinate formulation that can be easily calculated.

When the stiffness matrix $\mathbf{K}$ is constant, the strain energy has a simple expression, which is a quadratic form of the co-ordinates. This is not the case when the absolute nodal co-ordinates are employed, since the stiffness matrix is not a constant. Nevertheless, it is always possible to write the strain energy in the form

$$U = \tfrac{1}{2}\mathbf{e}^{\mathrm{T}}\mathbf{K}^{(U)}\mathbf{e}, \tag{91}$$

where the superscript (U) has been used to point out that, in general, the matrix $\mathbf{K}^{(U)}$ is not equal to the matrix $\mathbf{K}$.

6.1. LONGITUDINAL DEFORMATIONS

The expression of the strain energy U_l due to the longitudinal deformation can be written such that it resembles a quadratic form. Equation (91), written only for the longitudinal deformation, becomes

$$U_l = \tfrac{1}{2}\mathbf{e}^{\mathrm{T}}\mathbf{K}_l^{(U)}\mathbf{e}. \tag{92}$$

Substituting equation (32) into equation (20), it is possible to show that the matrix $\mathbf{K}_l^{(U)}$ is defined as

$$\mathbf{K}_l^{(U)} = \frac{1}{2}\mathbf{K}_l + \frac{EAl}{4}(\mathbf{I}_e - \bar{\mathbf{S}}_l). \tag{93}$$

In this equation, $\mathbf{K}_l$ is the stiffness matrix for longitudinal deformations, $\bar{\mathbf{S}}_l$ is the matrix defined by equation (30), and $\mathbf{I}_e$ is given by the diagonal matrix

$$\mathbf{I}_e = \frac{1}{8}\begin{bmatrix} 1/e_1^2 & & & & & & & \\ & 1/e_2^2 & & & & & & \\ & & 1/e_3^2 & & & & & \\ & & & 1/e_4^2 & & & & \\ & & & & 1/e_5^2 & & & \\ & & & & & 1/e_6^2 & & \\ & & & & & & 1/e_7^2 & \\ & & & & & & & 1/e_8^2 \end{bmatrix}, \tag{94}$$

where e_i are the element nodal co-ordinates. One can easily prove that $\mathbf{e}^{\mathrm{T}}\mathbf{I}_e\mathbf{e} = 1$. Equation (93) demonstrates that the strain energy can be written in a compact form, as in the case of linear structural mechanics. However, the matrix given by equation (93) is not suitable for numerical evaluation, because of the structure of the matrix $\mathbf{I}_e$. In order to numerically evaluate the strain energy, the following expression can be used:

$$U_l = \frac{1}{2}\left[\frac{1}{2}\mathbf{e}^{\mathrm{T}}\mathbf{K}_l\mathbf{e} + \frac{EAl}{4}(1 - \mathbf{e}^{\mathrm{T}}\bar{\mathbf{S}}_l\mathbf{e})\right]. \tag{95}$$

Equations (93) and (95) hold in the cases of small and large deformations. The matrix $\mathbf{K}_l$ depends on the model that is considered for the evaluation of the elastic forces.

6.2. TRANSVERSE DEFORMATIONS

When the simple Model T1 is used, there is no problem in finding an expression for the strain energy due to transverse deformations since the stiffness matrix $\mathbf{K}_t$ is constant. Consequently, it is possible to write

$$U_t = \tfrac{1}{2}\mathbf{e}^{\mathrm{T}}\mathbf{K}_t^{(U)}\mathbf{e}, \tag{96}$$

where the matrix $\mathbf{K}_t^{(U)}$ is equal to the matrix $\mathbf{K}_t$ of equation (75). When Model T2 is employed, the stiffness matrix is no longer constant. However, the expression of the strain energy remains simple. Substituting equation (84) into equation (23) and using the assumptions of Model T2, one obtains $\mathbf{K}_t^{(U)} = \mathbf{K}_{t1}$, where $\mathbf{K}_{t1}$ is given by equation (89).

7. NUMERICAL RESULTS

In this section, numerical results are presented in order to examine the performance of the elastic force models presented in the preceding sections. Different combinations of the Models L1, L2, L3, T1 and T2 shown in Table 1 are used. Model I is the simplest and it employs the Models L1 and T1. Model II includes the elastic forces defined by Models L2 and T1. Model III is the combination of Models L3 and T1, and Model IV is the combination of Models L2 and T2. The reason why Model T2 was not combined with Model L1 or L3 is that these longitudinal deformation models are obtained with the assumption of small deformation. Under this assumption, there is no difference in considering Model T1 or Model T2, as $\bar{f} \simeq 1$ and $\mathbf{K}_{t2} \simeq \mathbf{0}$. On the other hand, in the case of large longitudinal deformations, Model L2 should be used and combined with Model T2. In

TABLE 1

Combination of the elastic force models

Model	Longitudinal force model	Transverse force model
0	Linear elastic model as presented in reference [1, 3, 21]	
I	L1	T1
II	L2	T1
III	L3	T1
IV	L2	T2

choosing these model combinations, consistency of the assumptions was taken into consideration.

All these models, which are obtained using a continuum mechanics approach, are compared to the linear elastic model that employs a local frame for the finite element [1, 3, 21]. Two examples are considered in this section; the first is a pendulum free to fall under the effect of gravity, and the second is a four-bar mechanism with a very flexible connecting rod.

7.1. FREE FALLING PENDULUM

In this first example, the free falling of a very flexible two-dimensional beam under the effect of gravity is considered. The beam is connected to the ground by a pin joint at one end, as shown in Figure 3. The beam has a length of 1·2 m, a circular cross section with an area of 0·0018 m^2, a second moment of area of 1·215E − 08 m^4, a density of 5540 kg/m^3, and a modulus of elasticity of 0·700E + 06 Pa. In the original configuration, the beam is horizontal and has zero initial velocity. Two cases are considered in the analysis of the falling pendulum. In the first case, the beam is assumed to fall under the effect of gravity, while in the second case the beam is accelerated by increasing the gravity constant to 50 m/s^2.

Figure 4 shows the vertical position of the free end when 12 elements are used to represent the beam motion. As expected, due to the large deformation, Models I and III do not converge, and their results are not reported in this figure. The results of Models II and IV are almost identical, while Model 0 gives slightly different results. The CPU times for all these simulations are shown in Table 2.

When 40 elements are employed to study the same problem, all models converge, as shown by Figure 5. It is interesting to note that Models II and IV lead to the

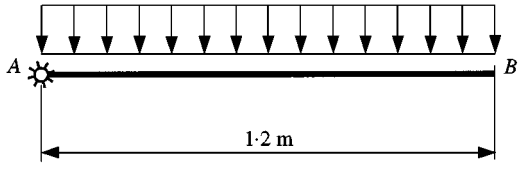

Figure 3. Free falling pendulum.

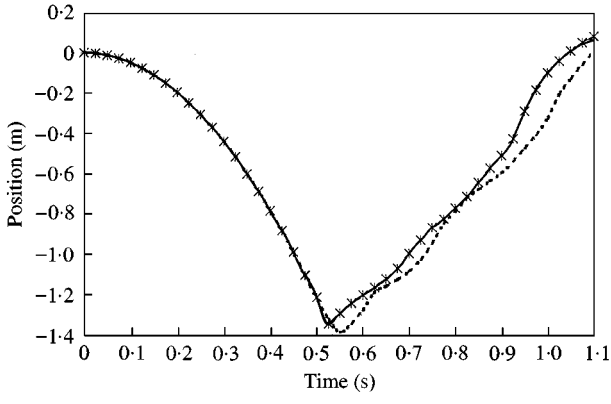

Figure 4. Vertical position of the free end of the pendulum using 12 elements: - - -, Model 0; —, Model II, −∗−, Model IV; $a = 9{\cdot}81\ m/s^2$.

TABLE 2

CPU times[†] and CPU time percentages with respect to Model 0

Simulation	Model 0	Model I	Model II	Model III	Model IV
Free falling pendulum, 9·81 m/s^2, 12 el.	6 (100%)	—	6 (100%)	—	7 (117%)
Free falling pendulum, 9·81 m/s^2, 40 el.	75 (100%)	34 (45%)	83 (111%)	60 (80%)	90 (120%)
Free falling pendulum, 50 m/s^2, 12 el.	9 (100%)	—	10 (111%)	—	12 (133%)
Free falling pendulum, 50 m/s^2, 40 el.	95 (100%)	—	126 (133%)	—	148 (156%)
Free falling pendulum, 50 m/s^2, 100 el.	1573 (100%)	1354 (86%)	2077 (132%)	1792 (114%)	2235 (142%)

[†] The CPU times (s) are obtained using a PC Pentium III 500 MHz. A value is reported only if the model converges for the whole simulation time of 1·1 s.

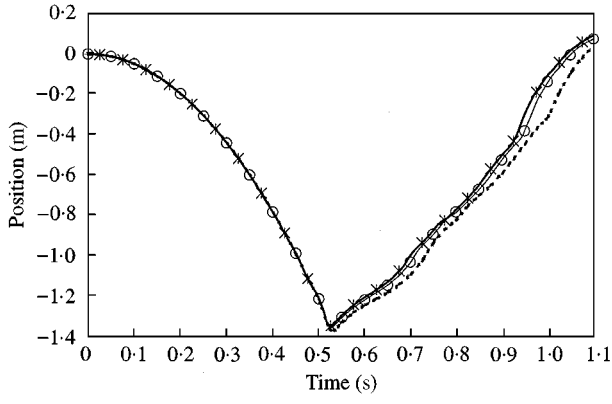

Figure 5. Vertical position of the free end of the pendulum using 40 elements: - - -, Model 0; —, Model I; —, Model II; ○, Model III; ∗, Model IV; $a = 9{\cdot}81\ \mathrm{m/s^2}$.

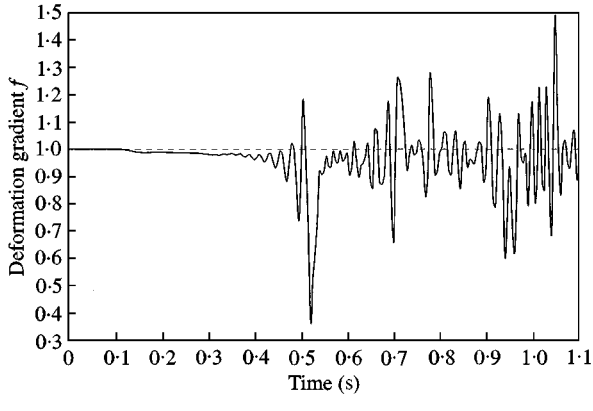

Figure 6. Deformation gradient f at the free end of the pendulum using Model I and 40 elements; $a = 9{\cdot}81\ \mathrm{m/s^2}$.

same results that have been obtained using only 12 elements. Furthermore, the results obtained using Model II are very close to the results of Model IV. Figure 6 shows the value of the deformation gradient f at the free end as a function of time. In this case, the deformation gradient is simply given by $\sqrt{e_3^2 + e_4^2}$, where e_3 and e_4 are the values of the slopes at the free end. As explained in Section 3, f should be equal to one in case of no deformation, and this also should be the case at the free end of the pendulum. Figure 6 shows the inaccurate results obtained using Model I, that employs an average value of the longitudinal strain throughout the finite element. Using the other models, this incorrect result is not obtained.

The free falling pendulum is a conservative system, and a simple energy analysis can be performed to demonstrate this fact. Three different types of energy are considered in this analysis: the kinetic energy T, the strain energy U and the potential energy V associated with the gravity forces. The kinetic energy T^i of the ith element is calculated as

$$T^i = \frac{1}{2}\int_0^{l^i} A^i \rho_0^i \dot{\mathbf{r}}^{iT} \dot{\mathbf{r}}^i \, \mathrm{d}x,$$

where l^i is the length, A^i is the cross-sectional area, and ρ_0^i is the density of the element. In this equation, $\dot{\mathbf{r}}^i$ is the time derivative of the global position vector of an arbitrary point on

the element. The strain energy U^i is calculated as the sum of the quantities U_l^i given by equation (95) and U_t^i given by equation (96). Using equations (8) and (9), the potential energy V^i due to the distributed gravity forces is defined as

$$V^i = g\int_0^{l^i} A^i\rho_0^i r_2^i \,\mathrm{d}x = m^i g y_G^i,$$

where m^i is the mass of the ith finite element, g is the gravity constant and y_G^i is the vertical position of the center of mass (positive upward). Since the system is conservative, the sum of these three energy types, evaluated for the whole system, should be constant:

$$\sum(T^i + U^i + V^i) = const.$$

In this case this constant is equal to zero for the given initial conditions. Figure 7 shows these three types of energy and the total energy as a function of time. The numerical results are obtained using Model II and 12 finite elements. It is interesting to note that the results obtained using 40 elements are almost identical. This example shows that the solution obtained with the absolute nodal co-ordinate formulation is consistent with the law of physics even though this is a problem of large deformations simulated using a relatively small number of elements (12).

Increasing the value of the acceleration constant to 50 m/s^2 results in a very large deformation. In this case, when 12 elements are used, the linear elastic Model 0 does not agree well with Models II and IV, as shown by Figure 8. As expected, using only 12 elements, Models I and III do not converge. The simulations of the pendulum that falls under the effect of an acceleration equal to 50 m/s^2 have been repeated using 40 elements. The results obtained are almost identical to the results previously presented in the case of 12 elements, and for this reason they are not presented. When 100 elements are employed for the same pendulum problem, Models I and III finally converge despite the large amount of deformation, as shown by Figure 9. This figure shows that Models I and III lead to very similar results, as well as the results of Model II are very close to the results of Model IV. As demonstrated by the motion animation shown in Figure 10, this example represents an extreme case of large deformation problem that involves high inertia forces. While Model 0 can be used to obtain a reasonable qualitative response in such an extreme case, as demonstrated by the result of Figure 9, a non-linear model can be used to obtain better

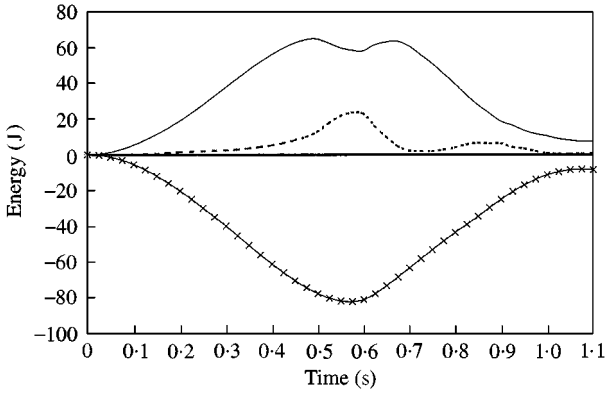

Figure 7. Energy balance for the free falling pendulum. Results obtained using Model II and 12 elements: - - -, strain energy; —, kinetic energy; –∗–, potential energy; —, total energy; $a = 9{\cdot}81$ m/s^2.

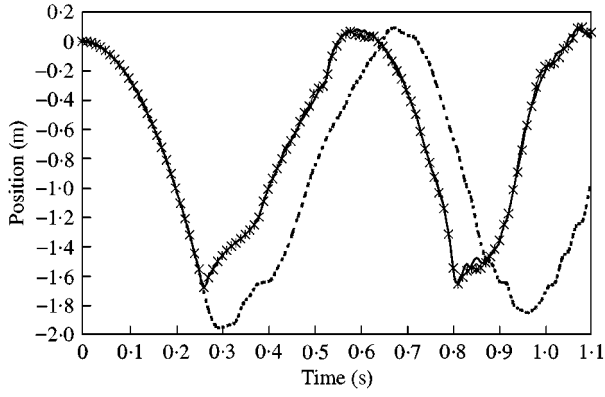

Figure 8. Vertical position of the free end of the pendulum using 12 elements: - - -, Model 0; —, Model II; −∗−, Model IV; $a = 50\ \mathrm{m/s^2}$.

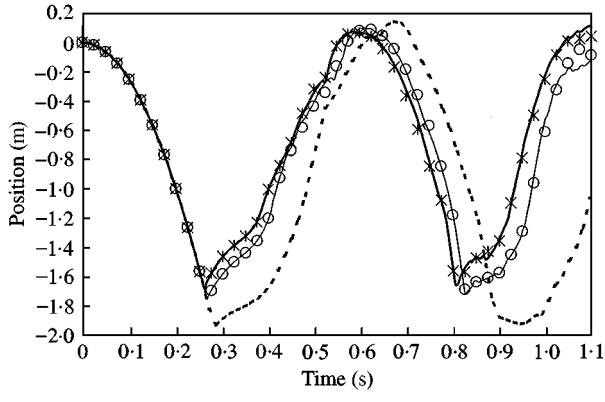

Figure 9. Vertical position of the free end of the pendulum using 100 elements: - - -, Model 0; —, Model I; —, Model II; ○, Model III; ∗, Model IV; $a = 50\ \mathrm{m/s^2}$.

convergence results. Nonetheless, Model 0, as demonstrated in the previous example and in the following example, converges to the correct solutions in many large deformation problems. The energy analysis, repeated for this case of increased value of the acceleration, gives results that are consistent with the principle of energy conservation, as shown by Figure 11.

7.2. FOUR-BAR MECHANISM

The four-bar mechanism considered in this second example is shown in Figure 12. The mechanism consists of a crankshaft, a connecting rod (coupler) and a follower. The mechanism is driven by a moment applied to the crankshaft. The driving moment is shown in Figure 13 as a function of time. The inertia, geometric, and elastic properties of the components of the four-bar mechanism are shown in Table 3. The table shows the mass m, the cross-sectional area A, the second moment of area I, the length l, and the modulus of elasticity E of the mechanism components. All components of the four-bar mechanism are assumed to be made of uniform beams which are initially straight. The gravity effect is taken into consideration. Pin joints are used to describe the connectivity conditions between the

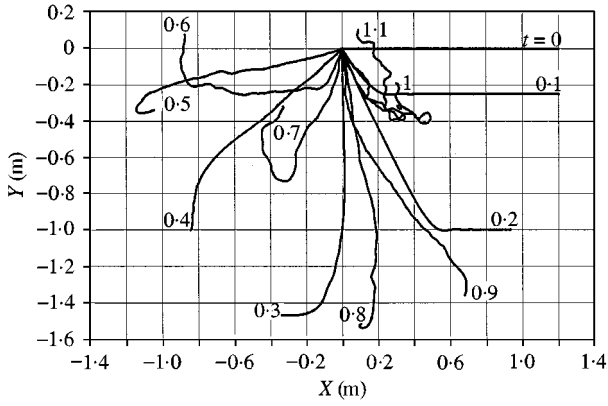

Figure 10. Configurations of the free falling pendulum at different times for the case $a = 50$ m/s^2 (values of time given in seconds).

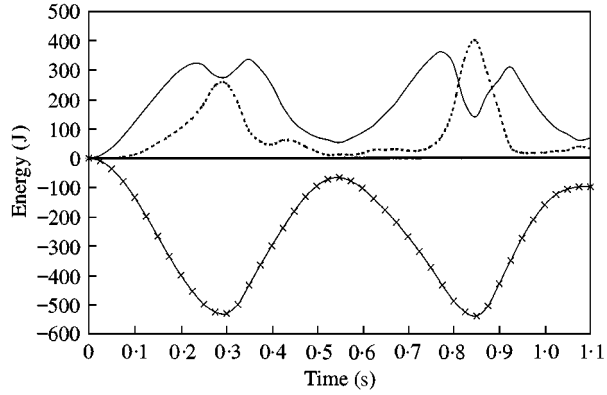

Figure 11. Energy balance for the free falling pendulum. Results obtained using Model II and 12 elements: - - -, strain energy; —, kinetic energy; −∗−, potential energy; —, total energy; $a = 50$ m/s^2.

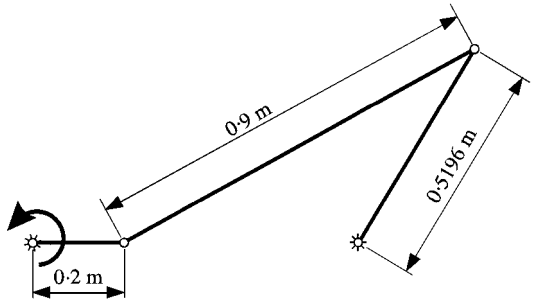

Figure 12. Four-bar mechanism.

components of the four-bar mechanism. The connecting rod of this mechanism is chosen to be very flexible, in order to allow for the large deformation.

In a first simulation model, 6 elements are used for the connecting rod, while only one element is used for the crankshaft and 4 elements are used for the follower. Therefore, the first simulation employs a total number of 11 elements. Figure 14 shows the transverse

TABLE 3

Parameters used in the simulation of the four-bar mechanism

Body	m (kg)	A (m^2)	I (m^4)	l (m)	E (Pa)
Crankshaft	0·6811	1·257E − 03	1·257E − 07	0·2	1·000E + 09
Coupler	2·4740	1·960E − 03	3·068E − 07	0·9	5·000E + 06
Follower	1·4700	7·068E − 04	3·976E − 08	0·5196152	5·000E + 08

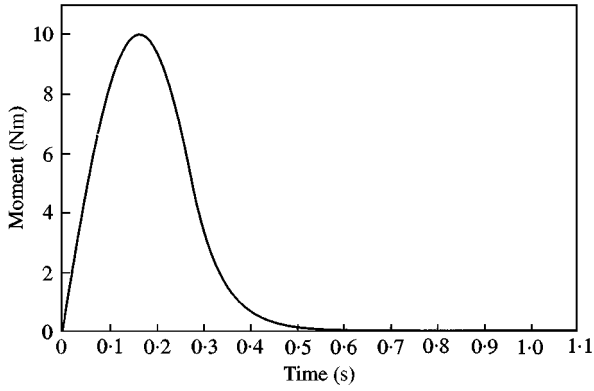

Figure 13. Moment applied to the crankshaft.

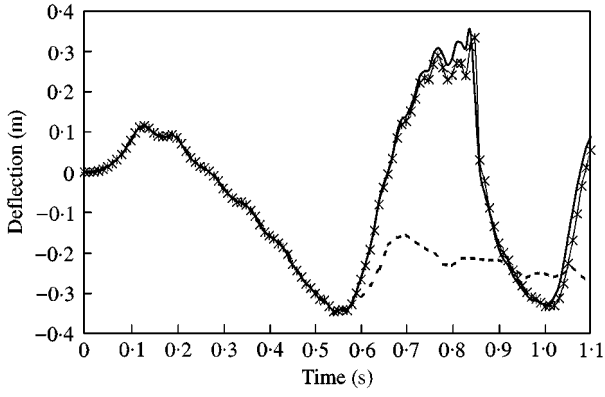

Figure 14. Transverse deflection of the midpoint of the crankshaft using 11 elements: - - -, Model 0; —, Model II; −∗−, Model IV.

deflection of the midpoint of the connecting rod using different models. The transverse deflection is determined as the distance of the midpoint to the straight line that connects the ends of the coupler. Due to the large amount of deformation, Models I and III do not converge. Models II and IV give very similar results, and Model 0 gives different results because of the small number of elements.

Another simulation is performed by increasing the number of elements of the connecting rod from 6 to 36, so that the total number of elements for the whole system is increased from 11 to 41. Figure 15 shows a comparison between the results obtained using all

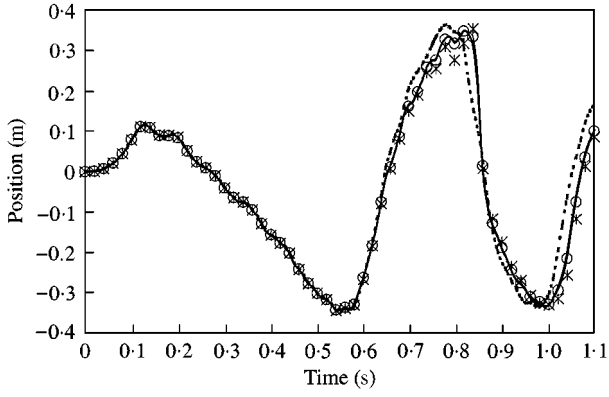

Figure 15. Transverse deflection of the midpoint of the crankshaft using 41 elements: - - -, Model 0; —, Model I; —, Model II; ○, Model III; ∗, Model IV.

the models for the transverse deflection of the midpoint of the connecting rod. All the results are in good agreement. The results obtained using Models II and IV and 41 finite elements are almost identical to the results obtained using the same models and 11 elements.

The four-bar mechanism driven by the moment shown in Figure 13 is not a conservative system. An energy analysis, however, can still be made, and the governing equation in this case is

$$\sum (T^i + U^i + V^i) = W,$$

where T^i, U^i and V^i are the kinetic energy, the strain energy and the potential energy, respectively, of the ith finite element, and W is the work performed by the driving moment. The sum is extended to all the elements of the system. The kinetic energy and the strain energy are defined as already shown in this section. The potential energy V^i is defined as

$$V^i = m^i g y^i_G - V^i_0,$$

where m^i, g and y^i_G have already been defined, and V^i_0 is a constant defined such that $V^i = 0$ for $t = 0$. The work W is calculated as

$$W = \int_0^{\theta(t)} M \, \mathrm{d}\theta,$$

where $\theta(t)$ is the rotation angle of the cross section of the crankshaft where the moment is applied. Figure 16 shows the different types of energy and the work done by the driving moment. It is clear that the results of the absolute nodal co-ordinate formulation are again consistent with the principle of work and energy. The performance of all the elastic force models in terms of computer time is shown in Table 4.

8. SUMMARY AND CONCLUSIONS

In this investigation, several models for the elastic forces due to the longitudinal and transverse deformation are developed for the use in the absolute nodal co-ordinate

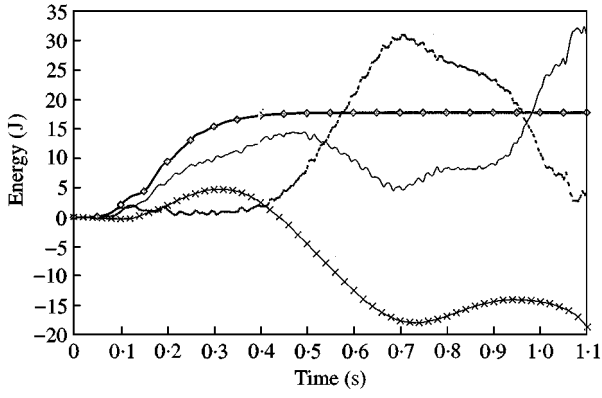

Figure 16. Energy balance for the four-bar mechanism. Results obtained using Model II and 11 elements: - - -, strain energy; —, kinetic energy; −∗−, potential energy; —, total energy; ◇, work.

TABLE 4

CPU times† *and CPU time percentages with respect to Model* 0

Simulation	Model 0	Model I	Model II	Model III	Model IV
Four-bar mechanism, 11 elements	148 (100%)	—	135 (191%)	—	165 (111%)
Four-bar mechanism, 41 elements	1615 (100%)	985 (61%)	1498 (193%)	1110 (69%)	1736 (107%)

† The CPU times (s) are obtained using a PC Pentium III 500 MHz. A value is reported only if the model converges for the whole simulation time of 1·1 s.

formulation. Two approaches can be used to formulate the elastic forces in the absolute nodal co-ordinate formulation. The first approach, which employs an element co-ordinate system, leads to a complex expression for the elastic forces even in the case of a linear elastic model [1]. A second approach based on a standard continuum mechanics procedure was recommended in reference [1] in order to obtain a much simpler expression for the elastic forces. It is the objective of this paper to show the significant simplifications that can be achieved by using the continuum mechanics approach. Several simple models that account for the effect of elastic nonlinearities due to the longitudinal deformations are presented. The assumptions used in developing these models are clearly stated and the advantages and drawbacks of these models are discussed. The results presented in this investigation also demonstrate the problems associated with the use of the linear elastic model when large deformation problems are considered. Because of the simplicity of the non-linear force models developed based on the continuum mechanics approach, significant saving in computer time could be achieved as compared to the force models developed using the local frame for the finite element based on a linear elastic model [1].

ACKNOWLEDGMENTS

This research was supported by the U.S. Army Research Office, Research Triangle Park, NC, and, in part, by the National Science Foundation.

REFERENCES

1. A. A. SHABANA 1998 *Dynamics of Multibody Systems*. Cambridge: Cambridge University Press, Second edition.
2. A. A. SHABANA 1996 *Technical Report No. MBS*96-1-*UIC*, *University of Illinois at Chicago.* An absolute nodal coordinate formulation for the large rotation and deformation analysis of flexible bodies.
3. A. A. SHABANA, H. HUSSIEN and J. ESCALONA 1998 *ASME Journal of Mechanical Design* **120**, 188–195. Application of the absolute nodal coordinate formulation to large rotation and large deformation problems.
4. T. J. R. HUGHES 1987 *The Finite Element Method*. Englewood Cliffs, NJ, Prentice-Hall.
5. M. CAMPANELLI, M. BERZERI and A. A. SHABANA 1999 *Technical Report No. MBS*99-2-*UIC*, *University of Illinois at Chicago.* Comparison between the absolute nodal coordinate formulation and incremental procedures.
6. C. C. RANKIN and F. A. BROGAN 1986 *ASME Journal of Pressure Vessel Technology* **108**, 165–174. An element independent corotational procedure for the treatment of large rotations.
7. O. A. BAUCHAU and N. K. KANG 1993 *Journal of the American Helicopter Society* **38**, 3–14. A multi-body formulation for helicopter structural dynamic analysis.
8. O. A. BAUCHAU 1998 *Multibody System Dynamics* **2**, 169–225. Computational schemes for flexible, nonlinear multibody systems.
9. M. BORRI and T. MERLINI 1986 *Meccanica* **21**, 30–37. A large displacement formulation for anisotropic beam analysis.
10. C. L. BOTTASSO and M. BORRI 1997 *Computer Methods in Applied Mechanics and Engineering* **143**, 393–415. Energy preserving/decaying schemes for non-linear beam dynamics using the helicoidal approximation.
11. A. CARDONA and M. GERADIN 1989 *Computers & Structures* **33**, 801–820. Time integration of the equations of motion in mechanism analysis.
12. A. CARDONA, M. GERADIN and D. B. DOAN 1991 *Computer Methods in Applied Mechanics and Engineering* **89**, 395–418. Rigid and flexible joint modelling in multi-body dynamics using finite elements.
13. J. C. SIMO and L. VU-QUOC 1986 *Computer Methods in Applied Mechanics and Engineering* **58**, 79–116. A three dimensional finite strain rod model. Part II: computational aspects.
14. J. C. SIMO, N. TARNOW and M. DOBLARE 1995 *International Journal for Numerical Methods in Engineering* **38**, 1431–1473. Non-linear dynamics of three-dimensional rods: exact energy and momentum conserving algorithms.
15. A. GOETZ 1970 *Introduction to Differential Geometry*. London: Addison Wesley Publishing Company.
16. S. TIMOSHENKO 1995 *Strength of Materials*. New York: Krieger Publishing Company, third edition.
17. K. WASHIZU 1968 *Variational Methods in Elasticity and Plasticity*. New York: Pergamon Press.
18. M. R. M. CRESPO DA SILVA 1988 *International Journal of Solids Structures* **24**, 1225–1234. Non-linear flexural-flexural-torsional-extensional dynamics of beams—I. Formulation.
19. J. MAYO, J. DOMINGUEZ and A. A. SHABANA 1995 *Journal of Vibration and Acoustics* **117**, 501–509. Geometrically nonlinear formulations of beams in flexible multibody dynamics.
20. Y. TAKAHASHI and N. SHIMIZU 1999 *Proceedings of the ASME Design Engineering Technical Conferences*, *Las Vegas*, *NV*. Study on elastic forces of the absolute nodal coordinate formulation for deformable beams.
21. J. L. ESCALONA, H. A. HUSSIEN and A. A. SHABANA 1998 *Journal of Sound and Vibration* **214**, 833–851. Application of the absolute nodal coordinate formulation to multibody system dynamics.